

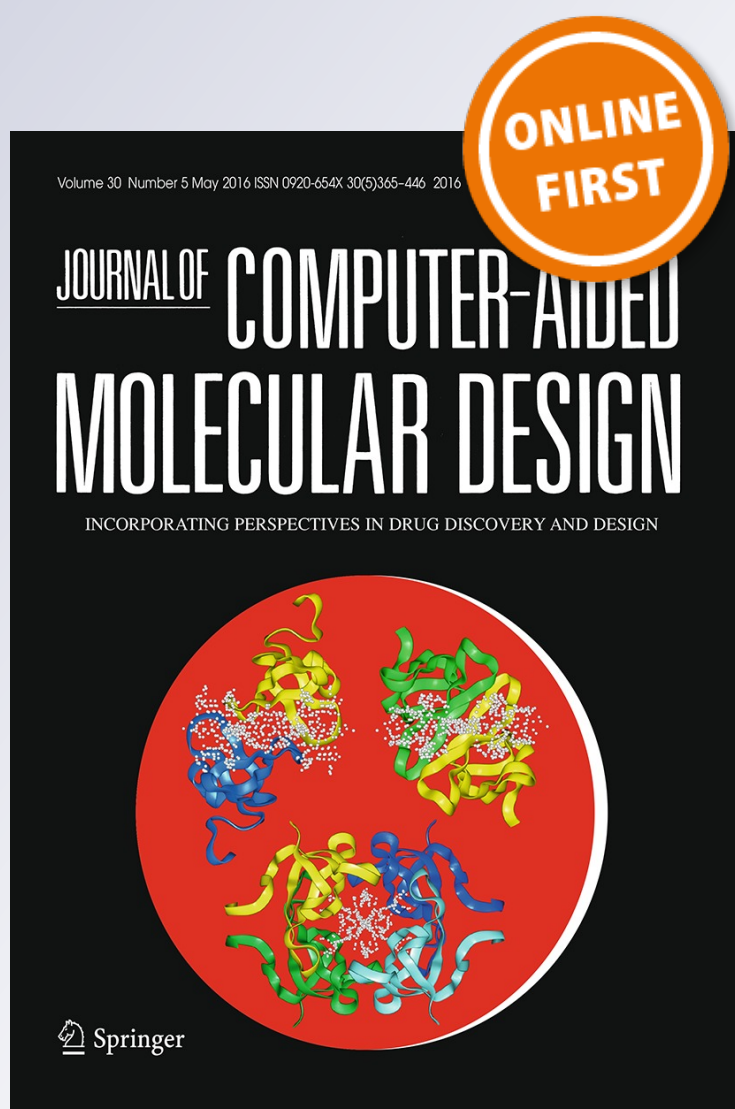
Computational study of the inhibitory mechanism of the kinase CDK5 hyperactivity by peptide p5 and derivation of a pharmacophore

**A. Cardone, M. Brady, R. Sriram,
H. C. Pant & S. A. Hassan**

**Journal of Computer-Aided
Molecular Design**
Incorporating Perspectives in Drug
Discovery and Design

ISSN 0920-654X

J Comput Aided Mol Des
DOI 10.1007/s10822-016-9922-3



Your article is protected by copyright and all rights are held exclusively by Springer International Publishing Switzerland (outside the USA). This e-offprint is for personal use only and shall not be self-archived in electronic repositories. If you wish to self-archive your article, please use the accepted manuscript version for posting on your own website. You may further deposit the accepted manuscript version in any repository, provided it is only made publicly available 12 months after official publication or later and provided acknowledgement is given to the original source of publication and a link is inserted to the published article on Springer's website. The link must be accompanied by the following text: "The final publication is available at link.springer.com".

Computational study of the inhibitory mechanism of the kinase CDK5 hyperactivity by peptide p5 and derivation of a pharmacophore

A. Cardone^{1,2} · M. Brady¹ · R. Sriram¹ · H. C. Pant³ · S. A. Hassan⁴

Received: 22 December 2015 / Accepted: 25 June 2016
© Springer International Publishing Switzerland (outside the USA) 2016

Abstract The hyperactivity of the cyclic dependent kinase 5 (CDK5) induced by the activator protein p25 has been linked to a number of pathologies of the brain. The CDK5–p25 complex has thus emerged as a major therapeutic target for Alzheimer's disease (AD) and other neurodegenerative conditions. Experiments have shown that the peptide p5 reduces the CDK5–p25 activity without affecting the endogenous CDK5–p35 activity, whereas the peptide TFP5, obtained from p5, elicits similar inhibition, crosses the blood–brain barrier, and exhibits behavioral rescue of AD mice models with no toxic side effects. The molecular basis of the kinase inhibition is not currently known, and is here investigated by computer simulations. It is shown that p5 binds the kinase at the same CDK5/p25 and CDK5/p35 interfaces, and is thus a non-selective competitor of both activators, in agreement with available experimental data in vitro. Binding of p5 is enthalpically

driven with an affinity estimated in the low μM range. A quantitative description of the binding site and pharmacophore is presented, and options are discussed to increase the binding affinity and selectivity in the design of drug-like compounds against AD.

Keywords CDK5 · p5 · p25 · p35 · TFP5 · Alzheimer's disease · Beta amyloid · Hyperphosphorylation · Protein–protein association · Computer simulation · Molecular dynamics

Introduction

The cyclin-dependent kinase 5 (CDK5) plays a central role in cognition, phosphorylation of cytoskeletal proteins, and other vital brain functions [1–3]. Under normal physiological conditions, CDK5 is regulated by neuron-specific activators p35 and p39. Under oxidative stress and other conditions, higher concentrations of Ca^{2+} activate the protease calpain, which cleaves p35 into fragments p25 and p10 [4–7]. The stable CDK5–p25 complex has a prominent role in the aberrant phosphorylation of tau proteins, which leads to the formation of β -amyloid plaques (BAP), neurofibrillary tangles (NFT), extracellular senile plaques of amyloid-42 (A), and intracellular NFT caused by accumulation of hyperphosphorylated proteins. Neuronal death is another consequence of CDK5 hyperactivity [4, 8, 9]. The CDK5–p25 complex has thus emerged as a major therapeutic target for Alzheimer's disease (AD) and other neurodegenerative conditions. The hyperactivity of CDK5 has been the focus of numerous studies, although effective therapeutic protocols are lacking. Drugs targeting BAP clearance [10, 11], cholinesterase inhibitors [12], and antioxidants to relieve oxidative stress [13, 14] have been

Disclaimer Commercial products are identified in this document in order to specify the experimental procedure adequately. Such identification is not intended to imply recommendation or endorsement by the National Institute of Standards and Technology or the National Institutes of Health, nor is it intended to imply that the products identified are necessarily the best available for the purpose.

✉ A. Cardone
antonio.cardone@nist.gov

¹ Software and System Division, National Institute of Standards and Technology, Gaithersburg, MD 20899, USA

² Institute for Advanced Computer Studies, University of Maryland, College Park, MD 20742, USA

³ Laboratory of Neurochemistry, NINDS, National Institutes of Health, Bethesda, MD 20892, USA

⁴ Center for Molecular Modeling, Division of Computational Bioscience, CIT, National Institutes of Health, Bethesda, MD 20892, USA

considered, but further studies are needed to assess their effectiveness and potential side effects. Inhibitors targeting ATP binding have also been considered, including aminothiazole and roscovitine [15–17], but they lack specificity as both aberrant and physiological activities are inhibited, leading to side effects and reduced therapeutic effectiveness.

A promising approach for the selective inhibition of CDK5–p25 is the use of small peptides obtained by truncation of p35 [18]. In vitro and in vivo data have shown that the truncated 24-residue peptide p5 specifically reduces CDK5–p25 activity, without affecting the endogenous CDK5–p35 function in presence of certain neuron specific molecules [7, 19]. A peptide derived from p5, TFP5, has recently been shown to cross the blood brain barrier and rescue cortical neurons without causing side effects [20]. This experimental evidence shows the potential of p5-based compounds to reach the brain and selectively inhibit the CDK5–p25 activity. However, the molecular basis of inhibition is not presently known, a problem exacerbated by the scarcity of structural information of p5 and the CDK5–p5 complex. This information is crucial to rationally design small peptide-mimetic drug-like compounds that can bind selectively and with high affinity to the same site(s) in the kinase.

The molecular basis of the inhibitory mechanism of p5 is here investigated by computer simulations. The study builds upon a series of recent developments on ab initio complex structure prediction [21, 22] and force field optimization [23–25]. The predicted binding modes suggest that p5 is a non-selective competitive inhibitor of p25, in accordance with available experimental data. Binding of p5 to the kinase is enthalpically driven with an affinity estimated in the low μM range. A quantitative description of a pharmacophore is presented, on the basis of which options are discussed to increase the binding affinity and specificity.

Results

The prediction of the CDK5–p5 complex structure in aqueous solution and at physiological conditions follows the general method described in [21, 22]. The method consists of three stages; in this case: (1) prediction of p5 and CDK5 conformers in solution; (2) identification of CDK5–p5 pre-relaxation binding modes; and (3) structural relaxation of the complexes at physiological conditions. The method makes no assumptions regarding geometric complementarity prior to binding, as both molecules can undergo structural changes upon contact. The method is thus designed to account for conformational selection of both molecules and for mutually induced fit upon

association. The method is also designed to identify weak and ultra-weak modes of association, which have been shown to play a role in molecular recognition [26, 27]. The method yields a set of conformational families of the complex, from which a discrete set of conformations (the “binding modes”) are identified. These modes are used to define the binding site(s) and possible pharmacophore(s). Application to the CDK5–p5 system makes use only of the amino acid sequence of p5 since its three dimensional structure in solution is unknown, and of the atomic coordinates of CDK5 in the active state, as obtained from the CDK5–p25 crystal [28].

Prediction of p5 conformers in solution

The amino acid sequence of the peptide p5 is $^1\text{KEAFWDRCLSVINLMSSKMLQINA}^{24}$, with both termini uncapped. All the residues are assumed to be neutral at pH 7 except K^+ , R^+ , E^- and D^- . The technique used to predict the conformers of p5 in solution has been described [23, 29]: first, a stochastic conformational optimization based on Monte Carlo Minimization/Annealing (MCMA) [29] simulations is performed to find a set of N structurally distinct low-energy conformations. Biased movements of side-chain or main-chain dihedral angles are generated and energy-minimized before a decision on acceptance is made. The N optimized conformations are used as initial structures in a series of Replica-Exchange (REx) Langevin Dynamic simulations. Replicas are distributed over temperatures in ascending order of energies, with the lowest energy assigned to the lowest temperature where data are collected (here, 37 °C). Simulations are carried out with the all-atom CHARMM force field [30] and the SCP implicit solvent model [23, 25, 31, 32]. The converged canonical distribution contains a large number of structures, which are clustered to obtain a discrete set of conformational families [22]. The clustering algorithm [33] assumes a maximum intra-cluster C_α -rmsd variance of 2 Å, which determines the number of families. Cutoff values used for clustering should in principle be chosen based the expected structural fluctuations around a given conformational state, and are thus system dependent. Order parameters and B-factors from proteins in the PDB suggest that these fluctuations are typically less than 1.5 Å. Molecular dynamics simulations, however, tend to yield larger structural fluctuations, partially due to the accuracy of current force fields to reproduce properties of the folded state. Therefore, slightly larger cutoffs are used here to avoid potentially spurious sub-states that would increase the computational cost unwarrantedly. All clusters with populations $>5\%$ are considered. A representative member of each family is then selected and identified as a conformer of p5. The calculation for p5 yields four

conformers (Fig. 1), each with relatively small populations but all sharing common structural motifs, similar to those of the same sequence in p25: a stable α -helix spanning residues K1–S10 and a less stable helix between I12 and A24; a kink around V11 may provide flexibility for fast interconversion. Each of the conformers has the potential to bind the kinase in a variety of modes and affinities and elicit specific biological responses.

Prediction of CDK5–p5 pre-relaxation binding modes

All the conformers of p5 are treated as independent structures coexisting in solution with conformers of CDK5. Unlike p5, for which a canonical ensemble could be obtained, thorough sampling of the conformational space of CDK5 is not feasible. However, the crystal structure of the CDK5–p25 complex (PDB ID: 1UNL) can be used to obtain a family of conformations in the vicinity of the active state of CDK5 through molecular dynamics simulations. The kinase was thus isolated from the crystal, immersed in water, and subjected to a 50-ns MD simulation at 37 °C and 1 atm (protocol described in section “[Structural relaxation and mutually induced fit](#)”). The trajectory was analyzed with the same clustering algorithm used for p5, using an intra-cluster C_{α} -rmsd variance of 2.5 Å. Two main conformational families were identified, each with about 50 % of the population. One family contains the active state, and its representative member is similar to the conformation of CDK5 in the complex. The conformer of the second family differs from the active conformer mainly in the activation loop. Further analysis of its dynamics indicates that this conformer does not represent a true (locally stable) sub-state, but results merely from transient fluctuations of the loop through the dynamics, probably on its path towards the transition state connecting the active and the inactive conformer of the kinase. In the latter case the activation loop adopts a stable retracted helical motif [34, 35], the structure of which is not known and is beyond

the reach of the present simulations. The focus in this study is on the inhibition of the active kinase and thus only the first conformer is used. The pharmacophore described in section “[Characterization of the pharmacophore](#)” is thus intended for targeting this active state. Other pharmacophores may eventually be developed for the inactive state.

The method used to predict the binding modes consists of two consecutive stages [21, 22]: a prescreening of favorable CDK5–p5 interactions aimed to identify physically relevant first-encounter modes, followed by a configurational biased sampling to identify statistically relevant conformational families of the complex. Both stages were described in detail previously [21, 22]; briefly, the prescreening consists of a simulated-annealing MC optimization of an electrostatic norm e and a hydrophobic norm h [21]. The functional forms of e and h are suitable simplifications of the physical effects that each one intends to describe, and they were designed specifically for computational efficiency: optimization of e represents electrostatic complementarity between the protein surfaces, whereas optimization of h represents the degree of burial of the local hydrophobic surfaces. No assumptions are made about surface complementarity because both proteins may undergo post-binding structural relaxations, and this is addressed in the final stage.

The prescreened modes are subsequently used to construct a biasing function for efficient conformational sampling using adaptive biased MC simulations with the complete force field. The resulting canonical distribution obtained upon convergence is post-processed by the clustering algorithm to identify a discrete set of binding modes using a cutoff of 2 Å. Simulations are carried out with the all-atom CHARMM force field [30] and the SCP implicit solvent model [23, 25, 31, 32]. The distributions of first-encounter modes (Fig. 2, upper row) are relatively broad but confined to specific regions of the kinase, most notably on the small domain. The calculations yield five structurally distinct CDK5–p5 binding modes (Fig. 2, middle row), with

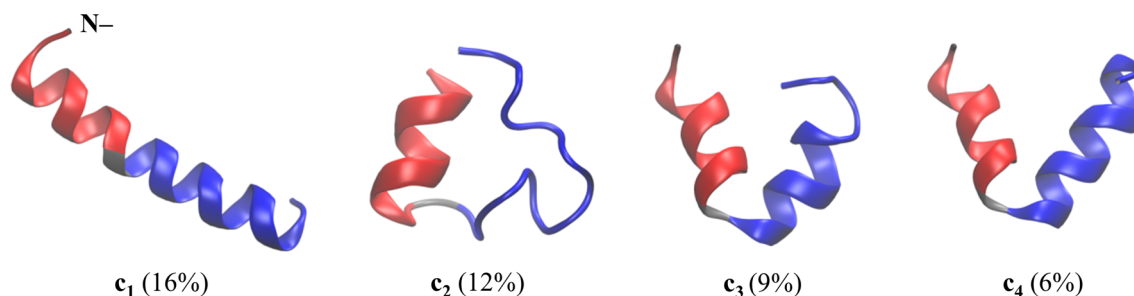


Fig. 1 Four predicted conformers of peptide p5 in aqueous solution at 35 °C and pH 7. Common structural motifs: K1–S10 α -helix (red), I12–A24 α -helix (blue), a kink around V11 (grey) may provide

flexibility for fast interconversion between conformers. Absolute populations indicated in *parentheses*

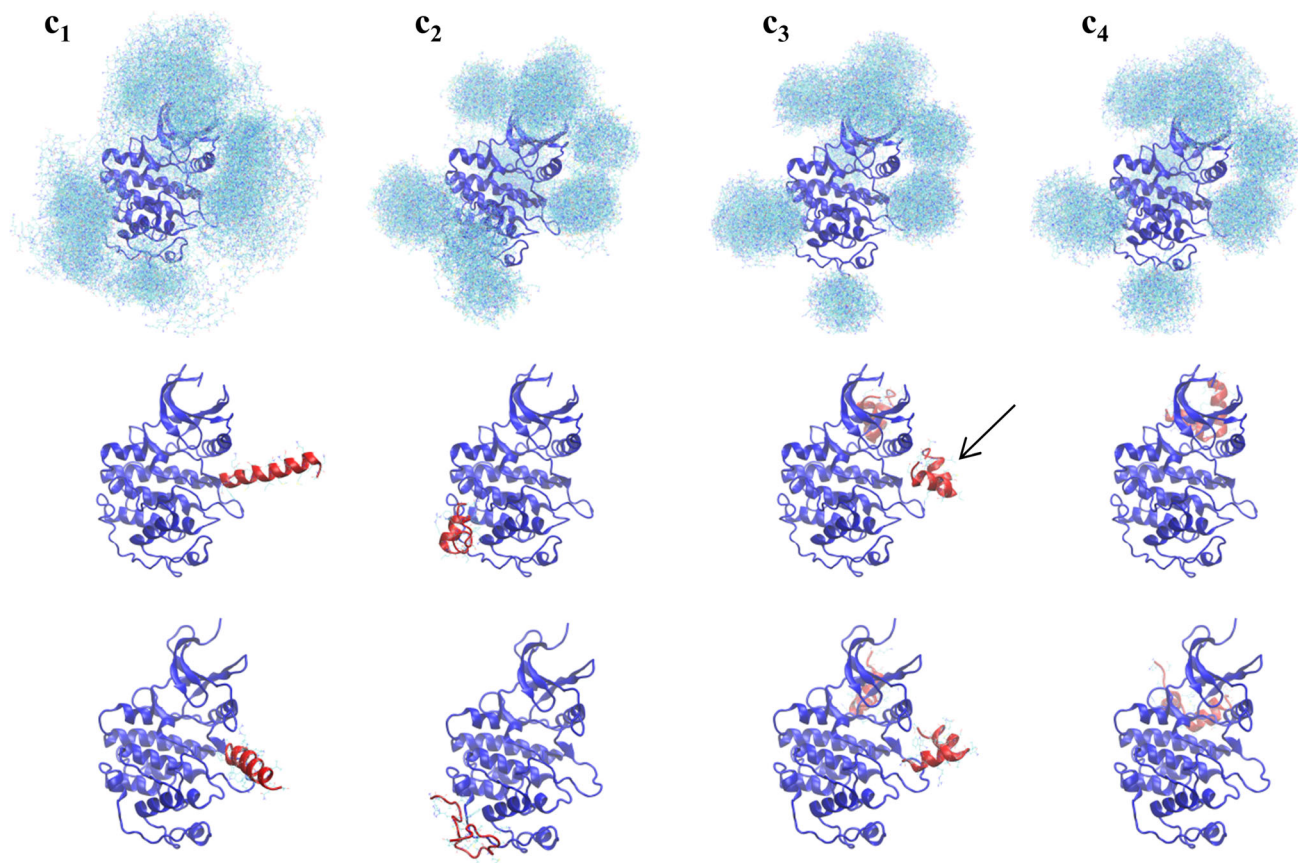


Fig. 2 Predicted CDK5–p5 complexes in aqueous solution at 35 °C: distribution of first-encounter modes (*top row*); pre-relaxation binding modes (*middle row*); and post-relaxation binding modes at

physiological conditions (*bottom row*). The *arrow* indicates the predicted inhibitory mode

one conformer (c_3) binding to two sites of the kinase. None of the modes appear to interfere directly with the ATP or the substrate binding sites. One of the modes (indicated by arrow) deserves special consideration since it binds the kinase at the known CDK5/p25 interface, and also at the predicted binding site of inhibitors p6 and CIP [22, 35, 36]. This site lies in the vicinity of three critical structural motifs implicated in both p25 and p35 binding and in the CDK5 activation and function [9, 18, 19, 28, 34, 35]: the PSAALRE helix (blue in Fig. 3), a loop rich in acidic residues (purple), and the activation loop (red). Unlike the other predicted binding sites, which may or may not be occluded by other proteins *in vivo* (e.g., the synaptic, vesicle-associated protein p67), this site is fully accessible to the solvent, hence to p5 or other inhibitors or activators. These observations suggest that inhibition of the aberrant CDK5–p25 hyperactivity by p5 (and presumably by TFP5 as well; cf. section “[Experimental evidence of selective and non-selective inhibition](#)”) can be explained as a competition for binding to the same site of the kinase.

To evaluate the strength of the CDK5–p5 interaction in this pre-relaxation inhibitory mode, the binding enthalpy

(ΔH) and binding entropy (ΔS) are calculated separately. The dissociation constant is given by $K_d = c^\ominus \exp(\Delta G/kT)$, where $c^\ominus = 1 \text{ M}$ is the standard concentration and $\Delta G = \Delta H - T \Delta S$ is the free energy of binding. Calculations are carried out at 37 °C using the all-atom CHARMM force field and the SCP solvent model. The enthalpy is calculated from the canonical distribution of the complex, obtained from a MC simulation [21, 22] as $\Delta H \approx \langle E_b \rangle - \langle E_\infty \rangle$, where $\langle E_b \rangle = Z^{-1} \sum_i E_i \exp(-E_i/kT)$ is the non-bonded energy of the bound state, Z is the partition function, k is the Boltzmann constant, and T is the absolute temperature; $\langle E_\infty \rangle$ is the non-bonded energy of the unbound complex. Trial moves consist of rigid-body rotations and/or translations, or rotations of a single side-chain torsion angle, and were carried out with a non-adaptive configurational-bias sampling [21]. The calculation yields $\Delta H \sim -10 \text{ kcal/mol}$, the largest value of the five modes. The entropy is given by $\Delta S = \Delta S_{rt} + \Delta S_c$, where ΔS_{rt} is the change in rotational–translational entropy upon binding, and ΔS_c is the corresponding change in configurational entropy, which include vibrational and (bond) rotational components. Based on previous studies [37, 38] the former

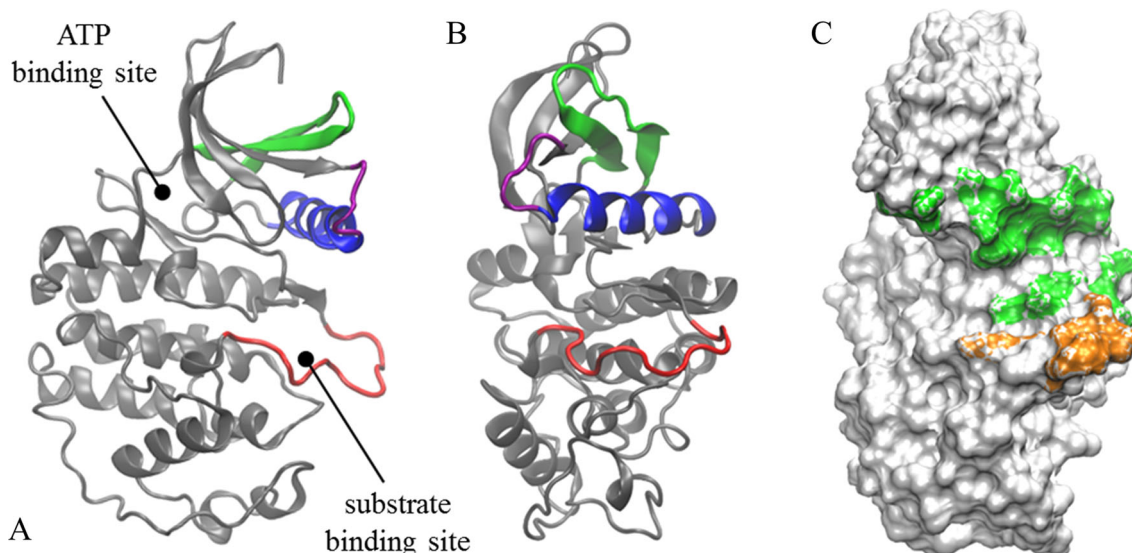


Fig. 3 **a** X-ray structure and **b** snapshot from the dynamics (rotated with respect to **a**): Ribbon representations of CDK5 showing key structural motifs involved in binding and regulation: acidic loop (purple), PSAALRE helix (blue), activation loop (red), and β -sheet structure of the small lobe (green); ATP- and substrate-binding pockets indicated. **c** Molecular surface of the CDK5 binding interface for the proposed inhibitory mode (same orientation as in **b**). Interfacial residues in contact with p5 obtained from six independent dynamics simulations shown in green and yellow (see text): D41,

E42, P45, S46, L49, R50, C53, L54, K56, E57, R120, N121, L123, R125, L147, R149, A150, F151, G152, I153, P154, V155, R156, Y158, S159. The interfacial residues corresponding to the other binding modes are: for c_1 : D39, G43, S46, R125, R149, V155, R156, C157, Y158, S159, E161; for c_2 : K213, R214, R217, L218, Y242, P243, T245, T246, N250, V251; for the non-inhibitory c_3 : K3, T26, E28, K59, H60, K61, R65; for c_4 : K59, H60, K61, N62, R65, K112, F116, C290

is here assumed to be $T\Delta S_{nr} \sim -2$ kcal/mol, whereas ΔS_c is calculated as the difference $\Delta S_c = S_b - S_\infty$, where S_b and S_∞ are the absolute configurational entropies of the complex in the bound and unbound states, respectively. These components are here estimated from the atomic fluctuations using the approximation [39] $S = k + k/2 \ln[\det(kT/h^2 \mathbf{M}\sigma + \mathbf{I}/12)]$ where \mathbf{M} and \mathbf{I} are the mass and unit matrices, and \hbar is the reduced Planck constant. The covariance matrix σ is obtained from Langevin dynamics simulations. Convergence of the cross-correlation terms is rather slow, so to speed up convergence the C_α atoms were fixed, and only the contribution of p5 were evaluated; even in this case simulations of 5–10 μ s length were required for convergence. The calculation yielded an unfavorable configurational entropy of about $T\Delta S_c \sim -1$ kcal/mol. The free energy of the solvent is incorporated into the energy function of the implicit model, so the solvent entropy is effectively embedded in the enthalpic contribution. In the SCP model the entropy is absorbed mainly in the cavity term and in the screening function, and is expected to be small; however, other solvent contributions not amenable to a mean field approximation may be important [21] and would require further analysis. The calculations then suggest that the initial binding of p5 to CDK5 is enthalpically driven and has an affinity in the μ M range; only a modest increase in affinity could be achieved by reducing the internal flexibility of the

ligand. A post-relaxation calculation, not conducted here, might yield a higher affinity due to structural adaptations at the surface and increased complementarity (cf. section “Structural relaxation and mutually induced fit”), although enthalpy–entropy compensation is always present and its effects are difficult to predict without additional studies.

Experimental evidence of selective and non-selective inhibition

In vivo and in vitro experiments [7, 19], have uncovered important aspects of AD-related CDK5 activity and hyperactivity. These include the selective inhibition of CDK5 hyperactivity by small peptides, such as p5, in the presence of neuron specific molecules. The results of the previous section imply that, in the absence of other proteins that could affect the predicted binding mode, p5 should inhibit both CDK5–p25 and CDK5–p35 activities similarly (non-selective inhibition). This conclusion is indeed supported by experimental data in vitro: in the absence of cytoskeletal or neuron specific molecules, such as p67, p5 displays similar inhibitory effects on the pathological and physiological activities. On the other hand, in the presence of p67, p5 selectively inhibits p25-induced deregulation and hyperactivity in vivo, showing only marginal effect on p35 activation (selective inhibition) [19]. Data were also obtained in vivo for TFP5, a modified, longer peptide

derived from p5: intraperitoneal injections of TFP5 on 5XFAD AD model mice show that TFP5 crosses the blood–brain barrier, whereas mice injected with TFP5 exhibited behavioral rescue with no toxic side effects [7]. Evidence of selective inhibition of abnormal CDK5 hyperactivity was also found. Additional *in vitro* kinase assays in presence of p67 and *in vivo* experiments on transfected Human Embryonic Kidney 293 (HEK 293) cells have confirmed the selective inhibition of CDK5 hyper-activity by TFP5 (to be published).

The available experimental evidence thus supports the notion that inhibition is non-selective in the absence of p67, and the inhibitory mode predicted here provides the molecular rationale for such non-selective behavior. On the other hand, in the presence of p67, both p5 and TFP5 inhibit the CDK5–p25 activity but not the CDK5–p35 activity in a dose-dependent manner. On the basis of these data it is proposed here that the 10-kDa N-terminal domain of p35 acts as a protector *in situ/in vivo*, possibly by shifting the thermodynamic equilibrium in favor of CDK5–p35 by interacting with p67 and/or microtubules. The molecular mechanism of this selectivity cannot be elucidated from the present study, as it requires an extension of the method to multi-protein systems [22].

Structural relaxation and mutually induced fit

The five predicted binding modes were subjected to dynamics simulations to analyze structural relaxation following the initial binding. The simulations were performed in the isothermal–isobaric ensemble at 37 °C and 1 atm; temperature and pressure were maintained with the Langevin and the Nosé–Hoover methods. The TIP3P water model and the all-atom CHARMM force field were used. The system was neutralized with Cl[−] ions, and ~150 mM of K⁺ and Cl[−] ions were added to mimic the intracellular ionic strength; residues R⁺, K⁺, E[−] and D[−] were assumed to be charged at pH 7, and protonation states were fixed throughout the simulations. Particle mesh Ewald summations and orthorhombic periodic boundary conditions were used; the simulation cells consisted of cuboids with dimensions chosen so that the minimum distance between protein images was ~4 nm. Additional specifications of the simulations were the same as reported previously [35]. The total simulation times varied between 30 and 50 ns, depending on the complex, and included an initial period of structural adaptation and at least 10 ns of structural stability, which were used for analysis. Six simulations were carried out for each binding mode for statistical purposes.

All the binding modes undergo conformational changes in various degrees. Figure 2 (bottom row) shows snapshots of the relaxed modes at the end of the simulations. The changes occur mainly in p5, and to a lesser extent in

unstructured segments of the small domain of CDK5; the large domain of the kinase remains largely unaffected, as observed previously in the dynamics of the CDK5–p25 and CDK5–CIP complexes [35]. The changes in p5 originate mainly in rearrangements of the helices, although partial unfolding is observed in some cases. The major changes in the complexes occur in the relative positions and orientations of p5 and CDK5, resulting in an increase in surface complementarity at the CDK5/p5 interface. This is more apparent in the inhibitory mode, which is here analyzed in more detail. Figure 3 shows the region on the surface of CDK5 corresponding to the CDK5/p5 binding interface for this binding mode. The surface includes all the atoms that are in contact with p5 at any point of the trajectories; a distance criterion is used to determine whether two atoms, *i* and *j*, are in contact, namely, if their separation *r* is such that no water molecule could fit in between (i.e., $r < 2.8 \text{ \AA} + R_{\text{vdw},i} + R_{\text{vdw},j}$). The interface includes residues (green) D41, E42, P45, S46, L49, R50, C53, L54, K56, and E57, all belonging to the acidic loop-PSAALRE helix sequence. In particular, residues E42 and R50 appear to be critical since they interact directly with p5 through hydrogen bonds (cf. section “[Characterization of the pharmacophore](#)”). Other interfacial residues (green) belong to the larger lobe, namely R120, N121, L123, and R125; and yet others (yellow) to the activation loop. Mutations of these interfacial residues are expected to change either the binding affinity, the selectivity, or the inhibitory activity of the complex in the presence of p5, and should then be the main focus of systematic mutagenesis studies to experimentally map the binding site. Mutations of CDK5/p5 interfacial residues of the other modes (listed in the caption of Fig. 3) would probe other possible inhibitory mechanisms, such as allosteric modulation of the kinase dynamics with potentially deleterious effect on ATP or substrate binding, as previously conjectured from results of dynamic simulations [35].

Characterization of the pharmacophore

The six independent dynamic simulations of the complex in the inhibitory mode were considered to propose a pharmacophore. Figure 4 shows the molecular-surface of a representative CDK5/p5 interface on both molecules taken from the equilibrated complex. Inspection of the surface electric field suggests strong polar interactions, indicated by circles on the molecules: two regions of negative potential on the surface of p5, formed mainly by the unprotonated carboxyl groups of the C-terminus (circle A) and the side chain of Glu2 (circle E), interact with regions of positive potential on the surface of CDK5, which involves the PSAALRE helix and the end portion of the activation loop. In addition, a region of positive potential

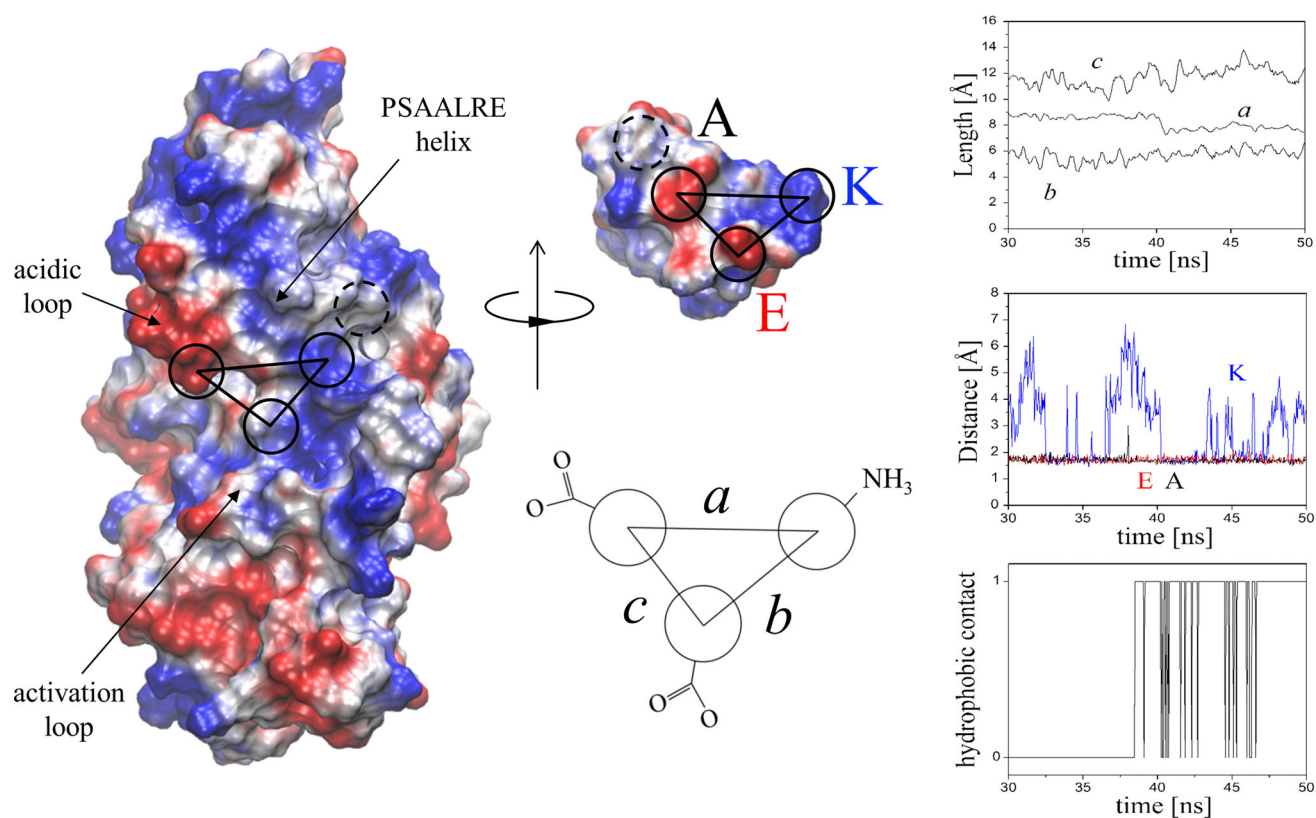


Fig. 4 Electrostatic representation on the molecular surface of the CDK5/p5 interface of the inhibitory mode (negative potential: red; positive: blue) indicating the regions of strong polar interactions inferred from the simulations (orientation similar to middle panel of Fig. 3). The view is obtained by rotating p5 in the direction indicated by the arrow. The main regions of electrostatic complementarity are denoted with solid circles A, E and K; a potentially relevant hydrophobic contact is shown with a dashed circle. A schematic representation of the main characteristics of the proposed pharmacophore is shown, in the same orientation as in p5 (see also Fig. 5). This pattern of interactions is reproduced in four out of six independent dynamics simulations; the average length among the

four simulations are in the ranges (in Å) $10 < a < 14$, $7 < b < 9$, and $6 < c < 8$; the right upper panel shows the time evolution in one of the four trajectories. The CO_2^- and NH_3^+ groups form persistent HB with CDK5 residues R50, R125, R149, R156, E42 and S159. The right middle panel shows the corresponding HB distances; the larger variations in K (NH_3^+) are due to the mobility of the lysine side chain, which transiently binds CDK5 by a water bridge; a more rigid molecule with the characteristics of the proposed pharmacophore should reduce these fluctuations. The frequency of hydrophobic contacts (dashed circles) is illustrated in the plot at the right lower panel (1, hydrophobic interaction; 0, otherwise)

on p5 formed mainly by the side chain of Lys1 (circle K), interact with a negative region on the surface of CDK5 formed by the acidic loop. A potentially relevant hydrophobic interaction (dashed circle) is also observed, which involves the same nonpolar region of the PSAALRE helix that stabilizes the CDK5–p25 complex. Equally important are the patterns of hydrogen bonds: one donor ($-\text{NH}_3^+$ of the Lys1 side chain) and one acceptor ($-\text{O}_2^-$ of the C-terminus and the Glu2 side chain) group in p5 interact with a reduced set of residues on the CDK5 surface (cf. caption of Fig. 4). To quantify these observations statistically, the hydrogen bonds and the contacts between the polar and between the non-polar moieties of p5 and CDK5 were calculated over the last 20 ns of the trajectories. In addition, the structural stability of p5 was confirmed through several internal RMSD measurements. Figure 4

(rightmost panels) shows the lengths a , b , and c in the proposed pharmacophore (lower middle panel) and the contact distances between the polar regions as a function of time in a typical simulation (see caption for details); the time evolution of the hydrophobic contacts is also shown (1 indicates hydrophobic interaction; 0 otherwise). These results are well reproduced in four out of the six simulations, thus statistically robust. Of the two outlier simulations, one still shows the same geometric and electrostatic pattern of the proposed pharmacophore but with longer sides a and c , whereas the second outlier shows larger structural distortions. These differences reflect the non-specific nature of p5 binding to CDK5, and the pharmacophore proposed here is expected to render the binding specific. Although the hydrophobic contact is observed in all the simulations, it is not included in the pharmacophore

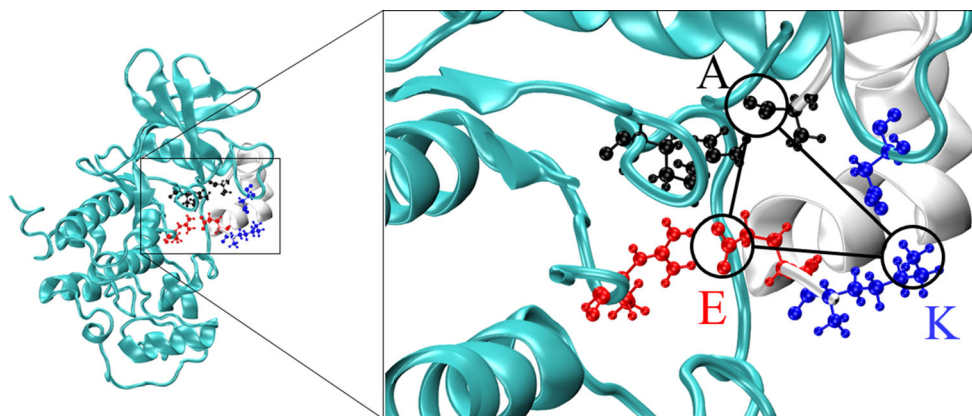


Fig. 5 Representation of the relative position of the pharmacophore of Fig. 4, showing p5 residues A, E and K hydrogen bonded with the corresponding partner residues in the kinase (obtained from a snapshot at the end of one of the simulations for schematic purpose).

since the electrostatic and the H-bond interactions appears to be strong enough for the stabilization of a prospective drug; other pharmacophores could, however, be proposed with a more hydrophobic character. Figure 5 shows schematically the pharmacophore in its three dimensional context, with an atomic representation of relevant interactions. Reproducing the pattern of interactions proposed in this pharmacophore appears to be feasible within the requirements of the Lipinski's guidelines (or variants thereof) for improved drug likeness, so the potential exists for replacing p5 (and TFP5) by a small, drug-like molecule that could elicit similar inhibitory effect on CDK5–p25 hyperactivity, thereby reversing β -amyloid deposition in AD.

Conclusions

The inhibitory mechanism of kinase CDK5 by the peptide p5 was investigated by computer simulations. A pharmacophore was described that can be used for the design of a small peptide-mimetic drug-like compound to target CDK5 and selectively inhibit the pathological CDK5–p25 hyperactivity. The study builds upon a series of recent developments on ab initio complex-structure prediction and force field optimization that allows detection and characterization of non-specific, sparsely populated binding modes of multi-conformer binding partners. The predicted binding modes suggest that p5 is a non-selective competitor of p25, and imply that both the physiological and the pathological activities are similarly inhibited in the absence of other proteins in the medium. This is consistent with available experimental data in vitro. The predicted binding site is located at the CDK5/p25 interface, and in the vicinity of three critical structural motifs implicated in p25 and p35 binding and in CDK5 activation and function,

Only residues interacting with p5 are shown in atomic detail. Due to conformational fluctuations, several other residues are found to transiently bind to p5 with statistically significant frequencies, as indicated in the caption of Fig. 4 (see text)

namely, the PSAALRE helix, the acidic loop, and the activation loop. It was shown that binding of p5 is generally non-specific, with a (pre-relaxation) affinity estimated in the low μM range, at most. The proposed pharmacophore is expected to make binding of a drug candidate more specific and increase its affinity. It was shown that enthalpy is the main contribution to binding ($\sim 70\%$), whereas configurational contributions to the binding entropy are small and unfavorable ($\sim 10\%$). Significant structural relaxations were observed upon association. Electrostatic and hydrogen-bond interactions are the main driving force to association and stability of the complex, whereas hydrophobicity seems to play a more modest role. Reproducing the predicted pattern of electrostatic/hydrogen-bond interactions may be feasible within the general guidelines for improved drug likeness, so p5 and, arguably, the longer peptide TFP5 can potentially be replaced by a small drug-like molecule that elicits similar inhibitory effect on CDK5 hyperactivity, thereby reversing β -amyloid deposition in AD. The current study provides the basis for systematic structure–activity studies.

Acknowledgments This study utilized the high-performance computer capabilities of the Biowulf PC/Linux cluster at the NIH. This work was supported by the NIH Intramural Research Program through the CIT and NINDS, and an internal NIST Research Fund.

References

1. Nikolic M, Dudek H, Kwon YT, Ramos YF, Tsai LH (1996) The cdk5/p35 kinase is essential for neurite outgrowth during neuronal differentiation. *Genes Dev* 10:816–825
2. Ohshima T, Ward JM, Huh CG, Longenecker G, Veeranna Pant HC et al (1996) Targeted disruption of the cyclin-dependent kinase 5 gene results in abnormal corticogenesis, neuronal pathology and perinatal death. *Proc Natl Acad Sci USA* 93:11173–11178

3. Tan TC, Valova VA, Malladi CS, Graham ME, Berven LA, Jupp OJ et al (2003) Cdk5 is essential for synaptic vesicle endocytosis. *Nat Cell Biol* 5:701–710
4. Ahljianian MK, Barrezueta NX, Williams RD, Jakowski A, Kowsz KP, McCarthy S et al (2000) Hyperphosphorylated tau and neurofilament and cytoskeletal disruptions in mice overexpressing human p25, an activator of cdk5. *Proc Natl Acad Sci USA* 97:2910–2915
5. de la Monte SM, Ganju N, Feroz N, Luong T, Banerjee K, Cannon J et al (2000) Oxygen free radical injury is sufficient to cause some Alzheimer type molecular abnormalities in human CNS neuronal cells. *J Alzheimer's Dis* 2:261–281
6. Patrick GN, Zukerberg L, Nikolic M, de la Monte S, Dikkes P, Tsai LH (1999) Conversion of p35 to p25 deregulates CDK5 activity and promotes neurodegeneration. *Nature* 402:615–622
7. Shukla V, Zheng YL, Mishra SK, Amin ND, Steiner J, Grant P et al (2013) A truncated peptide from p35, a Cdk5 activator, prevents Alzheimer's disease phenotypes in model mice. *FASEB J* 27:174–186
8. Lee MS, Kwon YT, Li M, Peng J, Friedlander RM, Tsai LH (2000) Neurotoxicity induces cleavage of p35 to p25 by calpain. *Nature* 405:360
9. Noble W, Olm V, Takata K, Casey E, Mary O, Meyerson J et al (2003) CDK5 is a key factor in tau aggregation and tangle formation in vivo. *Neuron* 38:555–565
10. Bard F, Cannon C, Barbour R, Burke RL, Games D, Grajeda H et al (2000) Peripherally administered antibodies against amyloid beta-peptide enter the central nervous system and reduce pathology in a mouse model of Alzheimer disease. *Nat Med* 6:916–919
11. Maier M, Seabrook TJ, Lazo ND, Jiang L, Das P, Janus C et al (2006) Short amyloid-beta (A β) immunogens reduce cerebral A β load and learning deficits in an Alzheimer's disease mouse model in the absence of an A β -specific cellular immune response. *J Neurosci* 26:4717–4728
12. Ritchie CW, Ames D, Clayton T, Lai R (2004) Meta-analysis of randomized trials of the efficacy and safety of donepezil, galantamine, and rivastigmine for the treatment of Alzheimer disease. *Am J Geriatr Psychiatry* 12:358–369
13. Bonda DJ, Wang X, Perry G, Nunomura A, Tabaton M, Zhu X et al (2010) Oxidative stress in Alzheimer disease: a possibility for prevention. *Neuropharmacology* 59:290–294
14. Lee HP, Zhu X, Casadesus G, Castellani RJ, Nunomura AS, Smith MA, Lee HG et al (2010) Antioxidant approaches for the treatment of Alzheimer's disease. *Expert Rev Neurother* 10:1201–1208
15. Helal CJ, Sanner MA, Cooper CB, Gant T, Adam M, Lucas JC et al (2004) Discovery and SAR of 2-aminothiazole inhibitors of cyclin-dependent kinase 5/p25 as a potential treatment for Alzheimer's disease. *Bioorg Med Chem Lett* 14:5521–5525
16. Helal CJ, Kang Z, Lucas JC, Gant T, Ahljianian MK, Schachter JB et al (2009) Potent and cellularly active 4 aminoimidazole inhibitors of cyclin-dependent kinase 5/p25 for the treatment of Alzheimer's disease. *Bioorg Med Chem Lett* 19:5703–5707
17. Knockaert M, Wieking K, Schmitt S, Leost M, Grant KM, Mottram JC et al (2002) Intracellular targets of paullones. Identification following affinity purification on immobilized inhibitor. *J Biol Chem* 277:25493–25501
18. Zheng YL, Kesavapany S, Gravel M, Hamilton RS, Schubert M, Amin ND et al (2005) A Cdk5 inhibitory peptide reduces tau hyperphosphorylation and apoptosis in neurons. *EMBO J* 24:209–220
19. Zheng YL, Amin ND, Hu YF, Rudrabhatla P, Shukla VK, Kanungo J et al (2010) A 24-residue peptide (p5), derived from p35, the cdk5 neuronal activator, specifically inhibits CDK5–p25 hyperactivity and tau hyperphosphorylation. *J Biol Chem* 285:34202–34212
20. Binukumar BK, Zheng YL, Shukla V, Amin ND, Grant P, Pant HC (2014) TFP5, a peptide derived from p35, a CDK5 neuronal activator, rescues cortical neurons from glucose toxicity. *J Alzheimer's Dis* 39:899–909
21. Cardone A, Pant H, Hassan SA (2013) Specific and non-specific protein association in solution: computation of solvent effects and prediction of first-encounter modes for efficient configurational bias Monte Carlo simulations. *J Phys Chem B* 117:12360–12374
22. Cardone A, Bornstein A, Pant HC, Brady M, Sriram R, Hassan SA (2015) Detection and characterization of nonspecific, sparsely-populated binding modes in the early stages of complexation. *J Comput Chem* 36:983–995
23. Hassan SA, Steinbach PJ (2011) Water-exclusion and liquid-structure forces in implicit solvation. *J Phys Chem B* 115:14668
24. Hassan SA, Mehler EL (2012) In silico approaches to structure and function of cell components and their assemblies: molecular electrostatics and solvent effects. In: Egelman E (ed) *Comprehensive biophysics*. Academic Press, New York
25. Hassan SA (2014) Implicit treatment of solvent dispersion forces in protein simulations. *J Comput Chem* 35:1621–1629
26. Tang C, Ghirlando R, Clore GM (2008) Visualization of transient ultra-weak protein self-association in solution using paramagnetic relaxation enhancement. *J Am Chem Soc* 130:4048
27. Johansson H, Jensen MR, Gesmar H, Meier S, Vinther JM, Keeler C et al (2014) Specific and nonspecific interactions in ultraweak protein-protein association revealed by solvent paramagnetic relaxation enhancements. *J Am Chem Soc* 136:10277–10286
28. Tarricone C, Dhavan R, Peng J, Areces LB, Tsai LH, Musacchio A (2001) Structure and regulation of the CDK5–p25(nck5a) complex. *Mol Cell* 8:657
29. Steinbach PJ (2004) Exploring peptide energy landscapes: a test of force fields and implicit solvent models. *Proteins* 57:665
30. Brooks BR, Brooks CL, Mackerell AD, Nilsson L, Petrella RJ, Roux B et al (2009) CHARMM: the biomolecular simulation program. *J Comput Chem* 30:1545
31. Hassan SA, Mehler EL, Zhang D, Weinstein H (2003) Molecular dynamics simulations of peptides and proteins with a continuum electrostatic model based on screened Coulomb potentials. *Proteins* 51:109–125
32. Hassan SA, Mehler EL (2005) From quantum chemistry and the classical theory of polar liquids to continuum approximations in molecular mechanics calculations. *Int J Quantum Chem* 102:986
33. Szekely GJ, Rizzo ML (2005) Hierarchical clustering via joint between-within distances: extending Ward's minimum variance method. *J Classif* 22:151–183
34. Mapelli M, Massimiliano L, Crovace C, Seeliger MA, Tsai LH, Meijer L et al (2005) Mechanism of CDK5/p25 binding by CDK inhibitors. *J Med Chem* 48:671
35. Cardone A, Hassan SA, Albers RW, Sriram RD, Pant HC (2010) Structural and dynamic determinants of ligand binding and regulation of cyclin-dependent kinase 5 by pathological activator p25 and inhibitory peptide CIP. *J Mol Biol* 401:478–492
36. Cardone A, Albers RW, Sriram RD, Pant HC (2010) Evaluation of the interaction of cyclin-dependent kinase 5 with activator p25 and with p25-derived inhibitor CIP. *J Comput Biol* 17:1–15
37. D'Aquino JA, Freire E, Amzel LM (2000) Binding of small organic molecules to macromolecular targets: evaluation of conformational entropy changes. *Proteins Struct Funct Genet* 41(S4): 93–107
38. Yu YB, Privalov PL, Hodges RS (2001) Contribution of translational and rotational motions to molecular association in aqueous solution. *Biophys J* 81:1632–1642
39. Andricioaei I, Karplus M (2001) On the calculation of entropy from covariance matrices of the atomic fluctuations. *J Chem Phys* 115:6289–6292